JOURNAL OF MATERIALS SCIENCE 33 (1998) 4791–4795

The effect of heating rate on the sintering of agglomerated $NaNbO_3$ powders

E. R. LEITE, M. A. L. NOBRE, M. D. RIBEIRO, E. LONGO
LIEC-DQ-UFSCar, P.O. Box 676, 13565-905, São Carlos, SP, Brazil
E-mail: dels@power.ufscar.br

J. A. VARELA
Instituto de Química, UNESP, P.O. Box 355, 14801-970, Araraquara, SP, Brazil

The effect of heating rate on the sintering of agglomerated $NaNbO_3$ powders, processed by the polymeric precursors method, was studied. The results showed that the presence of agglomerated powder leads to a heterogeneous microstructure, with bimodal grain size distribution, after sintering. Using a high heating rate, the sintering of agglomerated particles was inhibits, leading to a homogeneous microstructure, with single grain size distribution. © *1998 Kluwer Academic Publishers*

1. Introduction

Chemical methods for synthesizing ceramic powders have been used to obtain controlled stoichiometric phases, as well as to obtain fine particles and controlled morphology. Using fine particles can lead to a reduction of sintering temperature to obtain fine microstructure with low porosity. However, strongly agglomerated powders, obtained during the chemical synthesis, lead to heterogeneous microstructure after sintering [1, 2].

The polymeric precursors method, developed by Pechini [3], has been used to synthesize different policationic oxides such as: $ZrTiO_4$ [4], $SrTiO_3$ [5], $NaNbO_3$ [6], $BaTiO_3$ [7, 8] and superconductor oxides [9]. This method allows stoichiometry control and leads to nanometric particles. Nobre *et al.* [6] reported good sinterability of $NaNbO_3$ powders obtained from this method, leading to densities near theoretical. Recently Leite *et al.* [10] reported the particle growth kinetics during calcining of powders of $NaNbO_3$ and $ZrTiO_3$ obtained by the polymeric precursor method. They observed that the growth process occurs in two stages. For temperatures below 800 °C the particle growth mechanism and neck formation are associated with surface diffusion. For temperatures above 800 °C, both particle growth and strong agglomeration formation are controlled by the nanometric particle cluster densification and by neck size controlled particle growth mechanism.

The objective of this work is to analyse the effect of heating rate on the sintering of $NaNbO_3$ agglomerated powders processed by the polymeric precursors method, aimed to control the deleterious effect of the agglomerates on the final microstructure of the ceramic.

2. Experimental procedure

2.1. Powder synthesis and characterization

For the $NaNbO_3$ (NN) synthesis, niobium and sodium citrates were formed by dissolution of the precursor salts (niobium ammonium oxalate, $NH_4H_2[NbO(C_2O_4)_3].3H_2O$ and sodium nitrate, $NaNO_3$) in an aqueous solution of citric acid (the ratio of [citric acid] to the [Nb] + [Na] was 3.0 in mol). These citrate solutions were mixed (stoichiometry [Nb]/[Na] = 1.0) and after homogenization by magnetic stirring at 80 °C, ethylene glycol (mass ratio of 40/60 in relation of citric acid) was added to promote polymerization of the Nb and Na citrates by a polyesterification reaction. This polymerization was made in two stages, at 120 °C for 5 h for water elimination and at 250 °C for 2 h for solid resin formation. The resulting polymer was ground in a ball mill and calcined, with air flow, at 700 °C for 1 h. X ray diffraction showed a single phase powder of $NaNbO_3$. Particle characterization by surface area measurement, using the Brunaues–Emmett–Teller (BET) method, showed particles with surface area of 24 $m^2\ g^{-1}$ and particle size of 53 nm. Nitrogen adsorption/desorption results showed powder with mesopores (2–100 nm) and open porosity with cylindrical geometry. Pore size distribution, analysed by the (BJH) method [13], showed bimodal pore size distribution with most frequent pores of 19 nm and 31 nm, as observed in Fig. 1.

These results suggest that the powder is formed by agglomerates of nonometric particles.

2.2. Sintering process

Pellets ($\phi = 8$ mm, $h = 5$ mm) of NN powder was prepared by isostatic pressing at 100 MPa. Green densities of 57% of the theoretical density (TD) were attained. The sintering process was carried out in a dilatometer up to 1250 °C (Netzsch 402, Selb, Germany) using several constant heating rates (2 to 98 °C min^{-1}). For an isothermal sintering test, the samples were introduced into the preheated furnace at 1300 °C for 15 min and after sintering, the sample was taken out of the furnace

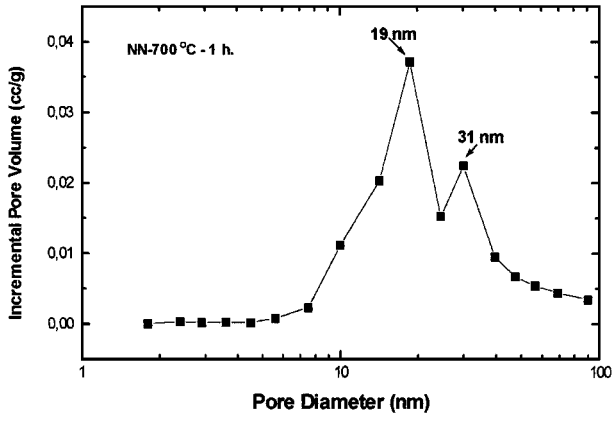

Figure 1 Pore size distribution, obtained by the N_2 isothermal desorption using BJH method, of the NN powder used in this study.

and cooled in air (5 min was sufficient for the furnace to attain equilibrium after introduction of the sample).

Microstructural characterization of the polished and thermally etched sintered samples were done by using a scanning electron microscope (SEM) (Zeiss, DSM 940, Germany).

3. Results and discussion

3.1. Sintering results

Linear shrinkage rates ($\mathrm{d}(\Delta L/L_\mathrm{o})/\mathrm{d}T$) as functions of temperature for the $NaNbO_3$ compacts are shown in Fig. 2 for different heating rates. All curves show two maximum peaks for different temperatures. A similar result was reported by Nobre *et al.* [6] where the low temperature peak is ascribed to the sintering of the agglomerates of nanometric particles. The displacement of the temperature of the maximum shrinkage rate (T^*) for higher values with increase of heating rate, for both peaks, is also observed in this figure.

The variation of temperature of the maximum shrinkage rate as a function of heating rate for both peaks, lower temperature peak (P_1) and higher temperature peak (P_2), is shown in Fig. 3. Displacements of both

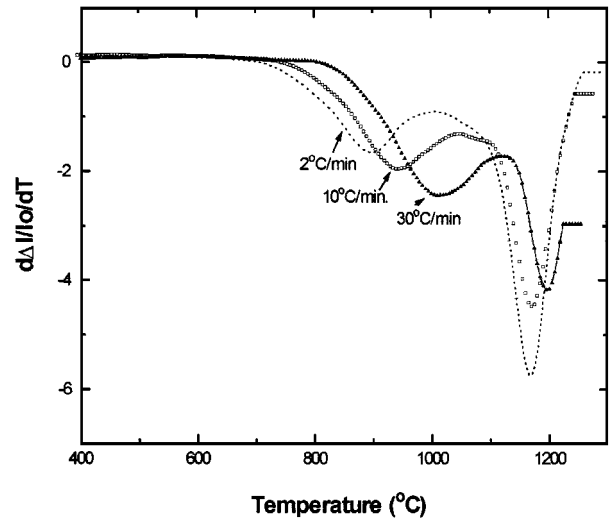

Figure 2 Linear shrinkage rate ($\mathrm{d}\Delta L/L_\mathrm{o}/\mathrm{d}T$) as a function of temperature, at several heating rates, for the NN powder calcined at 700 °C, for 1 h.

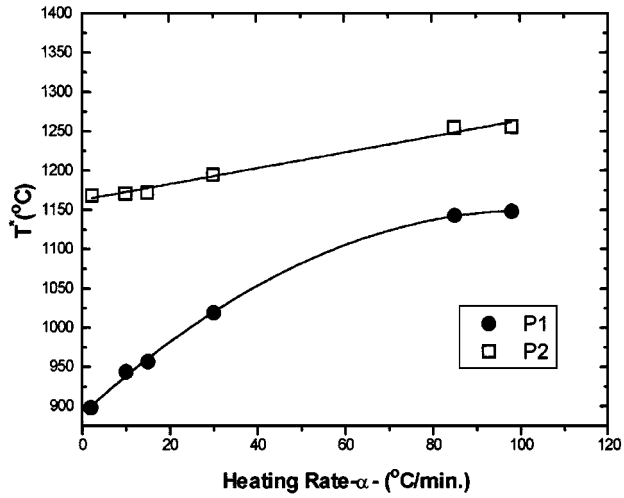

Figure 3 Temperature of maximum linear shrinkage rate (T^*) as a function of heating rate for both peaks, P_1 and P_2.

peaks to higher temperatures with the increasing heating rate are observed in this figure. However, the displacement of the peak P_1 is large, decreasing the temperature difference between both peaks. These results suggest that the densification of agglomerates are strongly dependent on the heating rate. Increasing the heating rate retards agglomerate densification, displacing the maximum shrinkage rate to higher temperatures.

Considering the equation derived by Kingery [11] for the isothermal linear shrinkage and modified by Jean and Gupta [12] for the constant heating rate sintering, the linear shrinkage rate is given by

$$\frac{\mathrm{d}(\Delta L/L_\mathrm{o})}{\mathrm{d}T} = \left(\frac{K_0^{1/n}}{nT\alpha^{1/n}}\right)\exp\left(\frac{-Q}{nRT}\right) \qquad (1)$$

where n is the exponent related to the mass transport, K_o is the pre-exponential constant, T is the Kelvin temperature, α is the heating rate, R is the gas constant and Q is apparent activation energy.

Considering the diferential of Equation 1 to the temperature T in both members

$$T\left[\frac{\mathrm{d}^2(\Delta L/L_\mathrm{o})}{\mathrm{d}T^2}\right] + \left[\frac{\mathrm{d}(\Delta L/L_\mathrm{o})}{\mathrm{d}T}\right] = \left[\frac{K_0^{1/n}}{n^2\alpha^{1/n}}\right)\left(\frac{Q}{RT^2}\right)\exp\left(\frac{-Q}{nRT}\right) \qquad (2)$$

For the temperature of maximum shrinkage rate (T^*) the second derivative as a function of T should be zero, that is, $\mathrm{d}^2\frac{(\Delta L/L_\mathrm{o})}{\mathrm{d}T^2} = 0$. Then, Equation 2 can be written for temperature T^* as

$$\left[\frac{\mathrm{d}(\Delta L/L_\mathrm{o})}{\mathrm{d}T}\right]_{T^*} = \left(\frac{K_0^{1/n}}{n^2\alpha^{1/n}}\right)\left(\frac{Q}{RT^{*2}}\right)\exp\left(\frac{-Q}{nRT^*}\right) \qquad (3)$$

Equation 3 predicts that increasing the heating rate increase the value of T^*, as observed in Fig. 3, as well as the reduction of $[\frac{\mathrm{d}(\Delta L/L_\mathrm{o})}{\mathrm{d}T}]$ for temperature $T = T^*$.

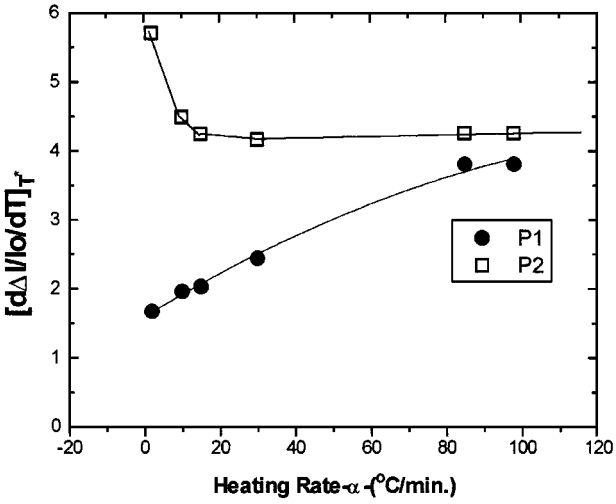

Figure 4 Linear shrinkage rate in $T = T^*$ as function of heating rate for both peaks, P_1 and P_2.

The plot $[\frac{d(\Delta L/L_o)}{dT}]_{T^*}$ as function of heating rate is shown Fig. 4. As predicted by Equation 3 there is a decrease in the value of maximum shrinkage rate as a function of heating, only for very slow rates, for the peak P_2 (related to the sintering of the particles). However, the maximum shrinkage rate for the peak P_1 (related to the sintering of agglomerates) increases with heating rate contrary with the prediction of Equation 3.

3.2. Microstructural evolution

The micrographs of Fig. 5 show the microstructure of the sodium niobate sintered in a dilatometer with a heating rate of 2 °C min^{-1} up to 1250 °C. The micrograph of low magnification (Fig. 5a) show a microstructure of low porosity with a series of grains pulled out during polishing. Using high magnification (Fig. 5b) a microstructure composed of two populations of grains is observed. One population is composed of fine grains with size ranging from 1 to 5 μm while the other population is composed of grains with size biger than 10 μm. Increasing the heating rate to 85 °C min^{-1} and sintering to the same final temperature, the microstructure also shows pulled out grains (Fig. 6a). The high magnification micrograph of this sample (Fig. 6b) indicates a bimodal distribution of grain size with the small grains preferentially pulled out by polishing. In both heating rate a microstructure formed by a fine grains embedded in a large grained matrix is observed.

The bimodal population of grain size should be related to the presence of agglomerates, in the starting powder, generating two maximum peaks in the shrinkage rate curve. Considering that the starting powder showed a primary mean particle size of 0.053 μm, the presence of large grain size (> 10 μm) indicates intensive grain growth during sintering. The presence of large grains can be associate with the densification of particle agglomerates originating polycrystalline grains. These polycrystalline grains will be transformed in large grains due to the displacement of grain boundaries. These large grains will induce secondary grain growth that will promote a final microstructure with coarse grains.

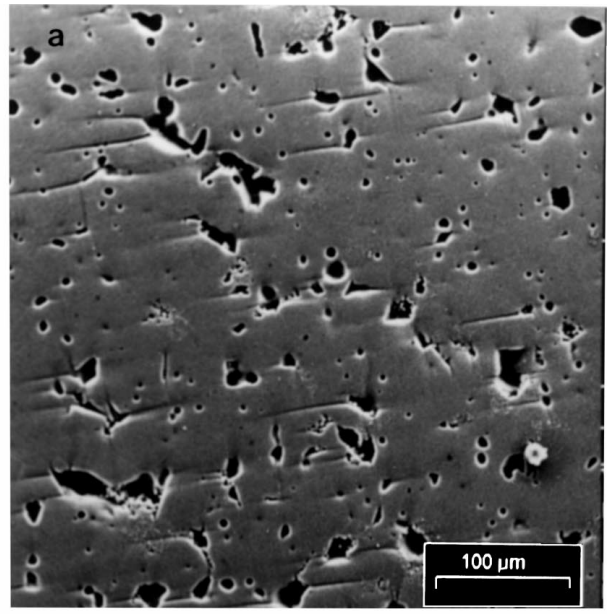

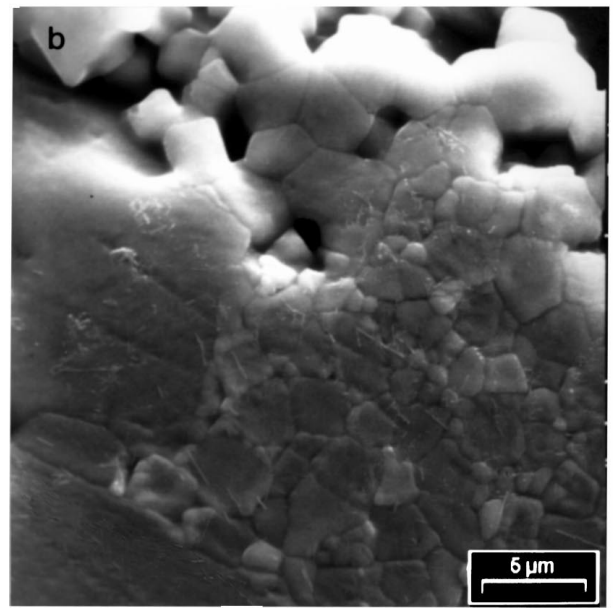

Figure 5 SEM micrographs of NN pellet sintered with a heating rate of 2 °C min^{-1}. (a) Low magnification; (b) high magnification.

3.3. General discussion

The results show that heating rate has a great influence on the agglomerates densification kinetics. The results of Fig. 3 indicate that both temperatures for the maximum shrinkage rates increase with increasing heating rate. The temperature difference between both peaks (P_1 and P_2) decreases with heating rate. Moreover, the results of Fig. 4 indicate that the maximum shrinkage rate in P_1 increases with heating rate while the maximum shrinkage rate in P_2 decreases with heating rate. These two maximum shrinkage rates reach similar value for higher values of heating rate. Microstructural analyses indicate that the presence of agglomerates promoted a microstructure with low porosity and a bimodal grain growth size distribution, with intensive grain growth, promoted by secondary grain growth.

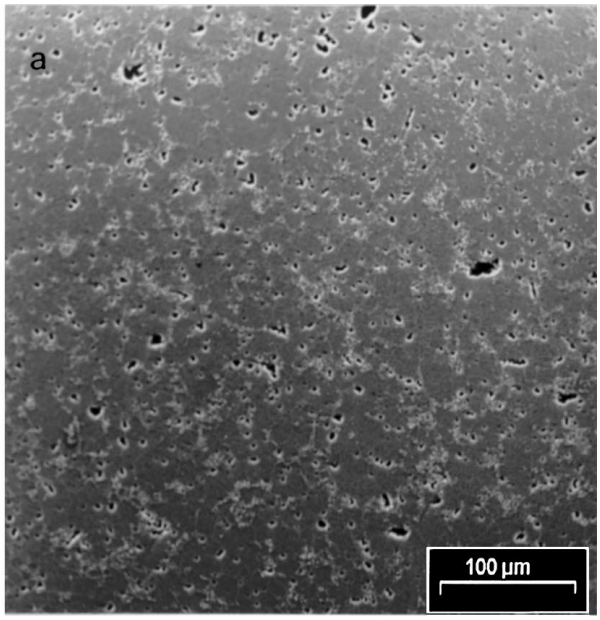

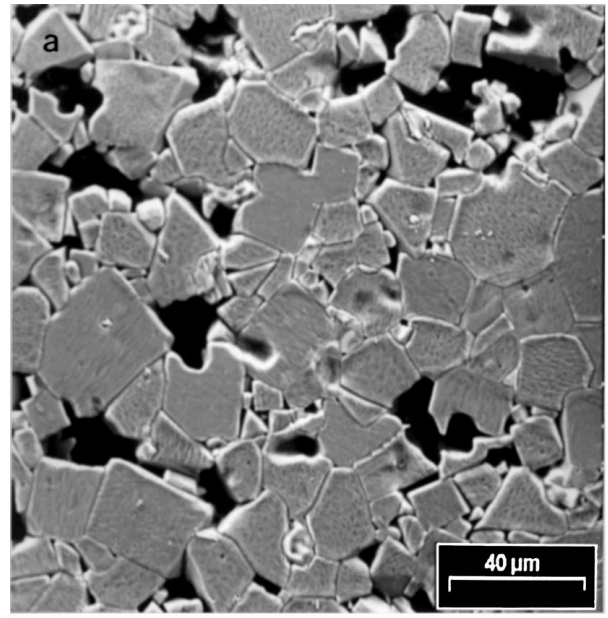

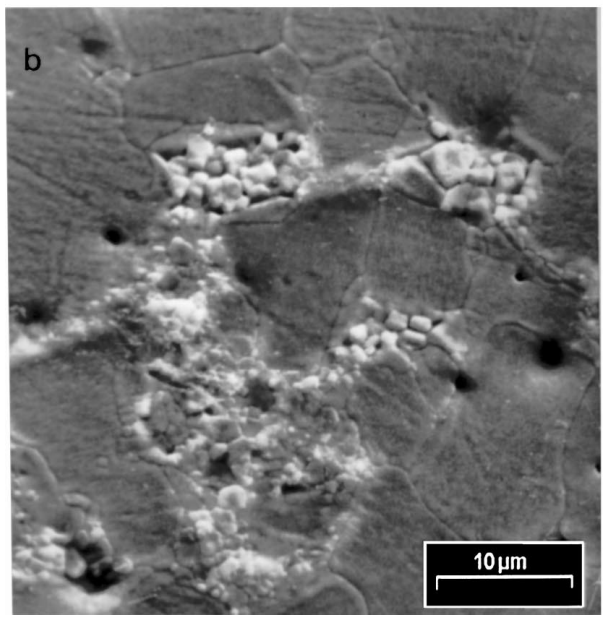

Figure 6 SEM micrographs of NN pellet sintered with a heating rate of 85 °C min^{-1}. (a) Low magnification; (b) high magnification.

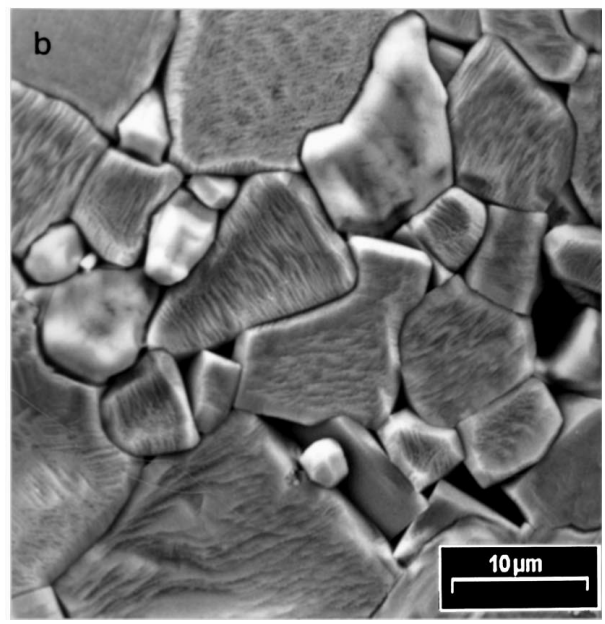

Figure 7 SEM micrographs of NN pellet isothermally sintered at 1300 °C for 15 min (a) low magnification (b) high magnification.

These results suggest that for a sufficient highly heating rate both the agglomerates and the individual particles would sinter with a similar shrinkage rate, resulting in an uniform microstructure with a single distribution of grain size. To verify this hypothesis the sintering of the samples in a very high heating rate was conducted in a tube furnace preheated to 1300 °C. The samples were rapidly put inside the hot zone and isothermally sintered for 15 min. A homogeneous microstructure was developed with a single distribution of grain size, as shown in Fig. 7. The use of a high heating rate should inhibit the preferential densification of agglomerates. However, the intensive grain growth, observed in the microstructure of Fig. 7 (mean grain size of 18 μm), is a indicative that the secondary grain growth process is not inhibit by the high heating rate.

As observed by Leite *et al.* [10] the sodium niobate agglomerate particles densify at temperatures above 800 °C. Using a high heating rate this process is retarded promoting the densification of agglomerates and non agglomerated particles at the same temperature. Using low heating rates the sintering process of sodium niobate occurs is two stages. In the first stage occurs the densification of agglomerates and in the second stage the non-agglomerated particles will densify. These results show that high heating rate or fast sintering can reduce the deleterious effect of agglomerates in the final microstructure, i.e. bimodal grain size distribution.

4. Conclusions

The experimental results of this work lead to the following conclusions:

1. The presence of agglomerates in sodium niobate powders formed by the polymeric precursors method leads to a heterogeneous microstructure with bimodal grain size distribution when compacts of this powder are sintered.

2. The sintering of agglomerates are strongly affected by the heating rate.

3. Fast sintering inhibits the preferential densification of sodium niobate agglomerates leading to a homogeneous microstructure with single grain size distribution.

Acknowledgements

The authors acknowledge CNPq, CAPES, FAPESP and FINEP, all Brazil agencies, for financial support and CBMM for supply the niobium ammonium oxalate.

References

1. C. LE CALVÉ-PROUST, E. HUSSON, P. ODIER and J. P. COUTURES, *J. Eur. Ceram. Soc.* (1993) 153.
2. C. MIOT, C. PROUST and E. HUSSON, *ibid.* **15** (1995) 1163.
3. M. P. PECHINI, US Patent no. 3.330.697 (1967).
4. M. CERQUEIRA, R. S. NASAR, E. LONGO, E. R. LEITE and J. A. VARELA, *Mater. Lett.* **22** (1995) 181.
5. E. R. LEITE, C. M. G. SOUZA, E. LONGO and J. A. VARELA, *Ceram. Int.* **21** (1995) 143.
6. M. A. L. NOBRE, E. LONGO, E. R. LEITE and J. A. VARELA, *Mater. Lett.* **28** (1996) 215.
7. S. KUMAR, G. L. MESSING and W. B. WHITE, *J. Amer. Ceram. Soc.* **76** (1993) 617.
8. M. ARIMA, M. KAKIHAMA, Y. NAKAMURA, M. YASHIMA and M. YOSHIMURA, *ibid.* **79** (1996) 2047.
9. M. KAKIHANA, *J. Sol–Gel Science and Tech.* **9** (1996) 7.
10. E. R. LEITE, M. CERQUEIRA, M. A. L. NOBRE, E. LONGO and J. A. VARELA, *J. Amer. Ceram. Soc.* **80** (1997) 2649.
11. W. D. KINGERY, *J. Appl. Phys.* **30** (1959) 301.
12. J. H. JEAN and T. K. GUPTA, *J. Mater. Res.* **7** (1992) 3342.
13. E. C. BARRET, L. G. JOYNER and P. P. HALENDA, *J. Amer. Chem. Soc.* **73** (1951) 373.

Received 28 November 1997
and accepted 17 July 1998